

## PERVASIVE LINEAR POLARIZATION SIGNALS IN THE QUIET SUN

L. R. BELLOT RUBIO<sup>1</sup> AND D. OROZCO SUÁREZ<sup>2</sup>

<sup>1</sup> Instituto de Astrofísica de Andalucía (CSIC), Apdo. 3004, 18080 Granada, Spain; lbellot@iaa.es and

<sup>2</sup> National Astronomical Observatory of Japan, 2-21-1 Osawa, Mitaka, Tokyo 181-8588, Japan

Received 2012 April 13; accepted 2012 July 3; published 2012 August 31

### ABSTRACT

This paper investigates the distribution of linear polarization signals in the quiet-Sun internetwork using ultra-deep spectropolarimetric data. We reduce the noise of the observations as much as is feasible by adding single-slit measurements of the Zeeman-sensitive Fe I 630 nm lines taken by the *Hinode* spectropolarimeter. The integrated Stokes spectra are employed to determine the fraction of the field of view covered by linear polarization signals. We find that up to 69% of the quiet solar surface at disk center shows Stokes Q or U profiles with amplitudes larger than 0.032% (4.5 times the noise level of  $7 \times 10^{-5}$  reached by the longer integrations). The mere presence of linear polarization in most of the quiet Sun implies that the weak internetwork fields must be highly inclined, but we quantify this by inverting those pixels with Stokes Q or U signals well above the noise. This allows for a precise determination of the field inclination, field strength, and field azimuth because the information carried by all four Stokes spectra is used simultaneously. The inversion is performed for 53% of the observed field of view at a noise level of  $1.3 \times 10^{-4} I_c$ . The derived magnetic distributions are thus representative of more than half of the quiet-Sun internetwork. Our results confirm the conclusions drawn from previous analyses using mainly Stokes I and V: internetwork fields are very inclined, but except in azimuth they do not seem to be isotropically distributed.

**Keywords:** magnetic fields – polarization – Sun: photosphere – Sun: surface magnetism

### 1. INTRODUCTION

There is growing evidence that quiet-Sun regions outside of the network—the so-called internetwork—are completely covered by magnetic fields. These fields appear to be weak and highly inclined to the vertical (e.g., Orozco Suárez et al. 2007b; Lites et al. 2008; Ishikawa & Tsuneta 2009; Asensio Ramos 2009; Borrero & Kobel 2011), but their characterization is challenging because they do not produce linear polarization signals of sufficient amplitude as to be measurable with the noise levels of current observations. Thus, important parameters such as the field inclination have been inferred rather indirectly, using Stokes I and V for the most part. While Stokes I and V are sensitive to the field inclination (del Toro Iniesta et al. 2010) and additional constraints can be obtained from the absence of Stokes Q and U, the fact is that without linear polarization the determination of the field inclination is difficult and subject to uncertainties (Asensio Ramos 2009; cf. Orozco Suárez & Bellot Rubio 2012).

To improve the inferences one has to analyze both circular and linear polarization signals at the same time. Using visible lines, however, Stokes Q or U are detected only in a small fraction of the surface area covered by the internetwork. For instance, the normal map and deep-mode *Hinode* observations of Lites et al. (2008) show clear linear signals (4.5 times the noise level or larger) in only 2% and 27% of the field of view, respectively (see Orozco Suárez & Bellot Rubio 2012). Even the more sensitive ground-based Fe I 630 nm measurements of Martínez González et al. (2008) do not go beyond 20%. The rest of the internetwork remains uncharted in linear polarization and may exhibit different magnetic properties.

The lack of detection of linear signals is due to the weakness of the fields. In the weak field regime, Stokes Q and U scale with the field strength  $B$  as  $B^2$  and Stokes V as  $B$ , so

weak fields generate linear polarization much less efficiently than circular polarization. Fortunately, Q and U are never zero except when the field is vertical, which opens the door to their detection by decreasing the noise of the measurements. Since internetwork fields appear to be highly inclined, linear polarization should exist almost everywhere in the quiet Sun, albeit with low amplitudes.

Here, we push the capabilities of current instruments to a limit in order to verify this conjecture. First, we combine the deep-mode observations of Lites et al. (2008) to improve their signal-to-noise ratio by up to a factor of 11. Once the noise is reduced, the measurements reveal clear linear polarization signals in most of the quiet-Sun internetwork. This corroborates the results of earlier analyses and puts them on a firmer basis. Second, we analyze the newly detected signals to determine the properties of internetwork fields very precisely. The derived properties apply to more than half of the internetwork surface area.

### 2. OBSERVATIONS

We use deep-mode observations taken by the spectropolarimeter (SP; Lites et al. 2001) of the Solar Optical Telescope (Tsuneta et al. 2008; Suematsu et al. 2008; Ichimoto et al. 2008; Shimizu et al. 2008) aboard *Hinode* (Kosugi et al. 2007). On 2007 February 7, the *Hinode* SP measured the full Stokes vector of the Fe I 630 nm lines with an exposure time of 9.6 s and a pixel size of  $0''.16$ . The  $160''$  long slit of the SP was kept fixed at disk center, sampling a very quiet region of the solar surface for 111 minutes. These observations have a noise level of  $8.0 \times 10^{-4}$  in units of the continuum intensity  $I_c$ .

To reduce the noise down to  $3.0 \times 10^{-4} I_c$ , Lites et al. (2008) added seven consecutive 9.6 s measurements, increasing the effective exposure time of the spectra to 67.2 s. After integration, 27% of the field of view showed Stokes Q or U signals above 4.5 times the noise level, a threshold considered suf-

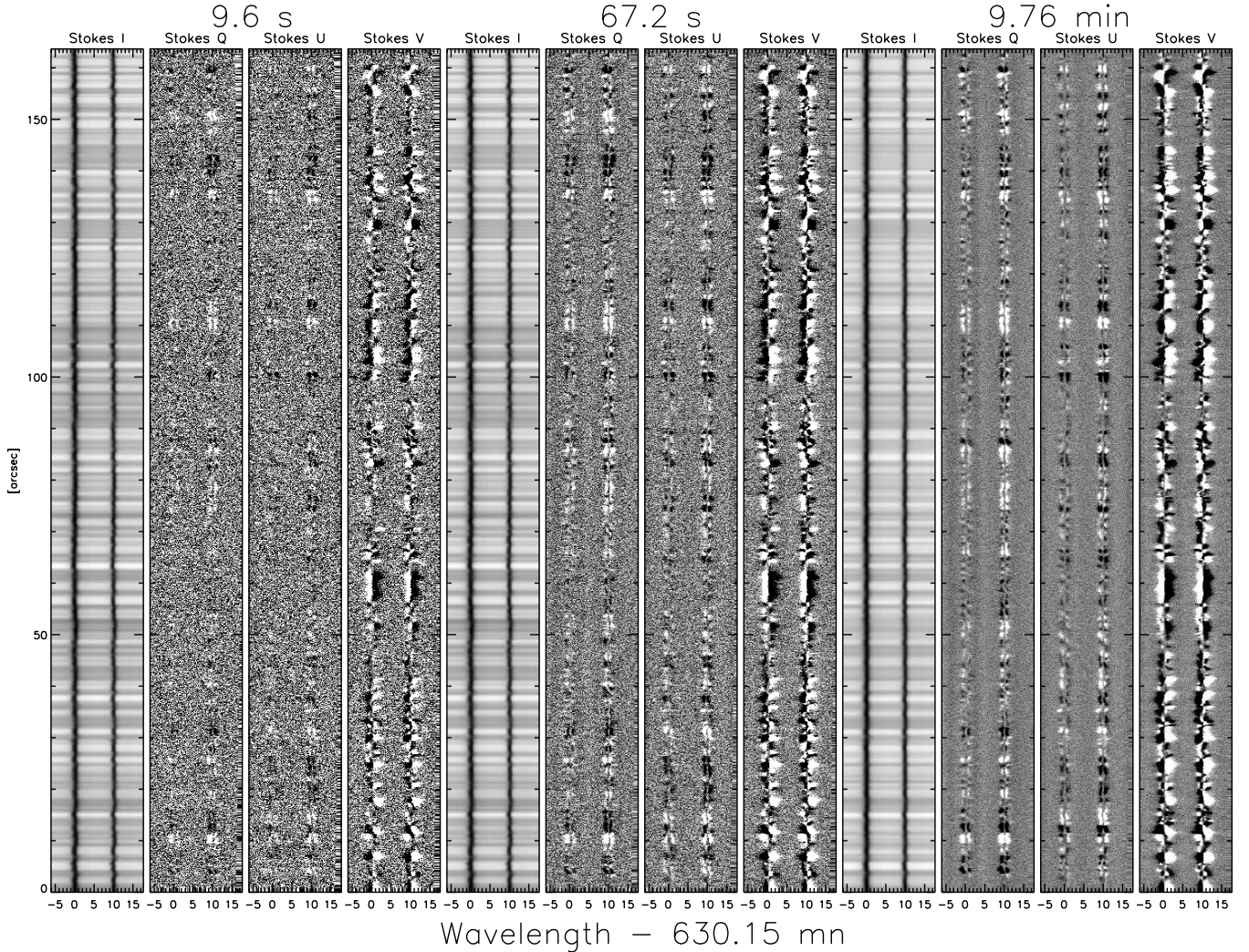


**Figure 1.** Stokes I, Q, U and V spectra along the slit for integration times of 9.6 s (left), 67.2 s (middle), and 9.8 minutes (right). The linear polarization signals (Stokes Q and U) stand out more prominently all over the slit as the integration time increases, i.e., as the noise decreases. The spatial resolution is degraded only slightly, as evidenced by the small changes in the intensity spectra.

ficient for meaningful analysis of the Stokes vector through Milne–Eddington inversions (Orozco Suárez & Bellot Rubio 2012). This percentage is much larger than the 2% found in *Hinode*/SP normal maps recorded with exposure times of 4.8 s and noise levels of  $10^{-3}I_c$  (Orozco Suárez & Bellot Rubio 2012), but still insufficient to fully characterize the quiet-Sun internetwork.

### 3. DATA ANALYSIS

Here, we exploit the idea of Lites et al. (2008) and continue the integration of the signals to decrease the noise level even further. By binning consecutive slits, we produce Stokes spectra with effective exposure times ranging from 9.6 s (1 slit—the original measurement) to 25.4 minutes (159 slits). Figure 1 shows an example of the signal-to-noise ratio gain in all the Stokes parameters, for integrations of 9.6 s, 67.2 s, and 9.8 minutes. One can clearly see that most of the polarization signals detected in the less noisy spectra (those on the right) are also present in the other panels, but virtually hidden by the larger noise. Thus, increasing the exposure time brings to view very weak signals which could not be observed before.

The variation of the noise with time is shown in the top

panel of Figure 2 (solid line). After 25 minutes of integration, the noise reaches an extremely low  $7 \times 10^{-5}I_c$  without the help of any filtering. The curve follows very closely the behavior expected for pure photon noise, indicating that other sources of uncertainty (e.g., CCD readout noise) are less important.

As the effective exposure time is increased, however, the spatial resolution of the spectra decreases due to changes in the solar scenery. The mean lifetime of granular cells is of the order of 5–15 minutes (Alissandrakis et al. 1987; Title et al. 1989; Hirzberger et al. 1999) and magnetic flux concentrations, with similar lifetimes<sup>1</sup>, are in constant motion buffeted by convective flows. Owing to the dynamical evolution of the solar surface, the superb spatial resolution of the *Hinode* SP is progressively degraded. We quantify this degradation through the rms contrast of the granulation in continuum intensity. The middle panel of Figure 2 shows the variation of the contrast with integration time. There is a steady decrease from 7.5% for integrations of 9.6 s to 4.2% for integrations

<sup>1</sup> The typical lifetime of the more horizontal internetwork fields is 1–10 minutes (Ishikawa & Tsuneta 2009; Danilovic et al. 2010). The more vertical internetwork fields live for 1.5–15 minutes, with a median value of 7.1 minutes (Gošić 2012).

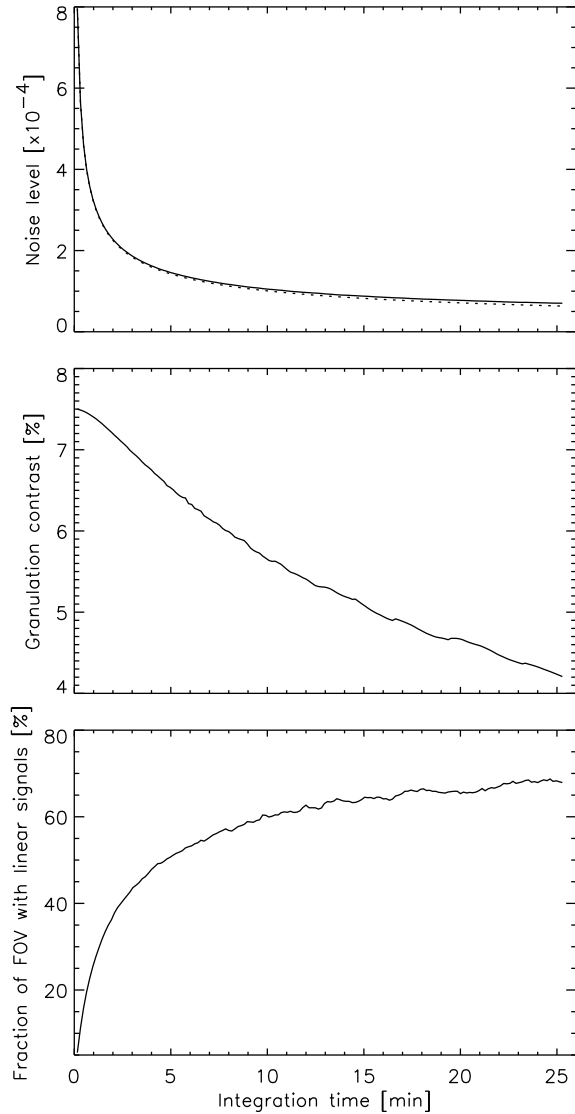


**Figure 2.** Top: noise level of the spectra vs. integration time (solid line). The noise is evaluated in the continuum of Stokes Q and U. The dotted line shows the reduction expected for photon noise, which is inversely proportional to the square root of the integration time. Middle: rms continuum contrast vs. integration time. Bottom: percentage of pixels with Stokes Q or U amplitudes above 4.5 times the noise level vs. integration time.

of 25 minutes, which is significantly longer than the typical granular lifetime. Still, these contrasts are higher than those obtained in ground-based observations with shorter exposure times<sup>2</sup>, which testifies to the stability of the instrument and the advantages of seeing-free observations from space.

The benefits of reduced noise levels are immediately apparent from the bottom panel of Figure 2. Shown there is the percentage of the field of view where we detect linear polarization (Stokes Q or U) above 4.5 times the corresponding noise level. The fraction of surface area covered by measurable lin-

<sup>2</sup> For example, the best granular contrast achieved with the Advanced Stokes Polarimeter during moments of excellent seeing was 3.5% (Lites 1996). With the help of adaptive optics, the Diffraction-Limited Spectropolarimeter reaches values of 5.2% in exposures of 4.3 s (Lites & Socas-Navarro 2004). The 27 s long observations of the Polarimetric Littrow Spectrograph analyzed by Khomenko et al. (2005) had an rms contrast of 2.7%.

ear polarization signals increases from about 5% to 69% as the effective exposure time varies from 9.6 s to 25 minutes. However, it is not necessary to go that far to see linear polarization in most of the internetwork: with integrations of 9.8 minutes, 60% of the pixels—nearly two-thirds of the total—already exhibit large Stokes Q and/or U amplitudes. The signals in the other pixels do not exceed  $4.5\sigma$ , but most of them are real as evidenced by their similar appearance in the two spectral lines and the fact that they often show up in Stokes Q and U simultaneously.

From this we conclude that the solar internetwork is pervaded by linear polarization signals.

#### 4. MAGNETIC PROPERTIES OF THE INTERNETWORK

We take advantage of the large fraction of pixels showing clear Stokes Q and U signals to derive the properties of internetwork fields with high precision. In particular, we are interested in inferring their strengths, inclinations, and azimuths. This is achieved by applying a Milne–Eddington inversion to the observed spectra, as done by Orozco Suárez et al. (2007b) and others (Orozco Suárez et al. 2007a,c; Borrero & Kobel 2011). The inversion determines nine free parameters characterizing the height-independent properties of the magnetized atmosphere within the pixel, plus the magnetic filling factor. The non-magnetic contribution in the pixel is modeled using a local intensity profile (Orozco Suárez et al. 2007c). According to Orozco Suárez & Bellot Rubio (2012), this treatment of the non-magnetic component in single-slit observations may slightly overestimate the field strength, but it does not affect the field inclination.

We choose to apply the inversion to the spectra integrated for 6.1 minutes. This is a compromise between high spatial resolution and complete coverage of the solar internetwork. We could have inverted the data with effective exposure times of 25 minutes, but at the cost of reduced spatial resolution. In order to maximize the chances that the same pixel samples the same solar structure during the integration time, we restrict ourselves to exposures of 6.1 minutes, which show both high spatial resolution and large surface coverage: 53% of the pixels in the data set exhibit clear Stokes Q or U signals with amplitudes larger than 4.5 times the noise level (of  $1.3 \times 10^{-4} I_c$ ), and 88% have Stokes V signals above the same threshold. Thus, the analysis of these observations is representative of more than half of the internetwork surface area, preserving most of the spatial resolution offered by *Hinode*.

As an example, Figure 3 displays the inversion results for a pixel with Stokes Q signals just above the  $4.5\sigma$  criterion. Note the extremely low noise level and the quality of the fit, which captures the essential properties of the observed spectra. In this case, the inversion indicates a magnetic field strength of 200 G, a field inclination of  $103^\circ$ , an azimuth of  $130^\circ$ , and a magnetic filling factor of 0.2. The Milne–Eddington inversion cannot reproduce the small asymmetries of the observed profiles because of the assumption of height-independent atmospheric parameters. As pointed out by Viticchié & Sánchez Almeida (2011), most of the profiles recorded by the *Hinode* SP are asymmetric to a larger or smaller degree. The asymmetries carry a great deal of information, whose extraction requires more complex inversion schemes (e.g., Socas-Navarro et al. 2008; Viticchié et al. 2011; Sainz Dalda et al. 2012). For the exploratory purposes of this study, however, a Milne–Eddington inversion is sufficient.

Figure 4 displays the time sequence of continuum intensity,

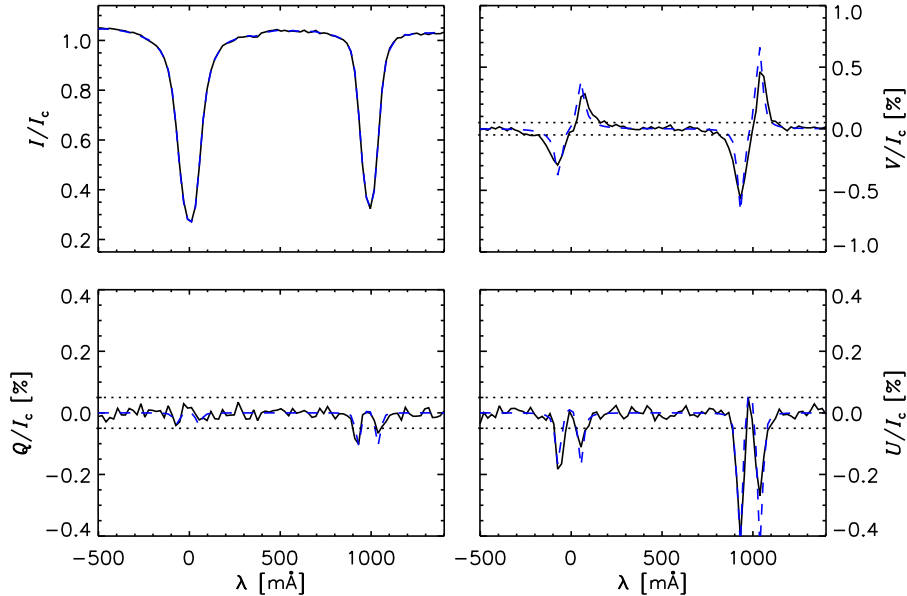


**Figure 3.** Example of observed Stokes profiles (solid) and best fit resulting from a Milne–Eddington inversion (dashed). The observed profiles correspond to an integration of 6.1 minutes and show Stokes Q signals just above 4.5 times the noise level.

circular, and linear polarization degrees for the 6.1 minute integration, as well as the field strengths, inclinations, and azimuths resulting from the inversion. The horizontal axis represents distance along the slit, while the vertical axis represents time (from bottom to top). Each row within the panels corresponds to an integration of 6.1 minutes. Despite the long effective exposure time, one can clearly distinguish small-scale flux concentrations which evolve in a coherent and smooth manner. For example, the proper motions of the structures produce inclined streaks in the panels. Interestingly, the circular and linear polarization maps show patches of comparable size in the horizontal direction (the spatial direction), all over the slit. Figure 5 illustrates this result. A different behavior was seen in the normal maps of the *Hinode* SP and the filtergrams acquired by IMA<sub>X</sub> (Martínez Pillet et al. 2011), the vector magnetograph of SUNRISE (Solanki et al. 2010; Barthol et al. 2011). Those instruments suggested a quiet-Sun internetwork consisting of relatively large circular polarization patches covering most of the surface and smaller, transient linear polarization patches that appear and disappear continually (Lites et al. 2008; Danilovic et al. 2010). The long integrations displayed in Figure 4 uncover much weaker signals, with the result that the size of the linear polarization patches increases (probably because their outer parts start to be detectable now).

Most of the structures seen in circular and linear polarization are recognizable in the field strength, inclination, and azimuth maps of Figure 4. Only the largest circular signals happen to be associated with fields stronger than 500 G, which are also the most vertical ones. The linear signals come from weak and very inclined fields. It is interesting to note that the azimuths show a smooth pattern in both spatial and temporal directions. The existence of structure in the azimuth map demonstrates the very precise determination of the three magnetic field components allowed by the small noise of the linear polarization profiles.

To obtain the distribution of field strengths, inclinations, and azimuths we only consider the 10,419 pixels having Stokes Q or U amplitudes larger than 4.5 times the noise

level<sup>3</sup>. They account for 53% of the quiet-Sun internetwork. The noise of  $1.3 \times 10^{-4} I_c$  reached by the 6.1 minute integration is equivalent to a polarimetric sensitivity of 0.2 G in longitudinal field and 15 G in transverse field<sup>4</sup>.

Figure 6 displays the resulting probability density functions (PDFs). As can be seen in the top panel, the field strength distribution peaks at 110 G, with a fast decrease toward stronger fields. No hump is detected at kG fields. The distribution also decreases rapidly toward 0 G. This appears to be a robust feature of the inversion, not caused by the noise of the profiles or the selection criteria<sup>5</sup>.

The central panel of Figure 6 reveals an inclination distribution dominated by horizontal fields (inclinations are measured from the local vertical). The PDF has a sharp maximum at  $90^\circ$ , with tails toward more vertical fields decreasing very quickly. Thus, in addition to purely horizontal fields, one also finds inclined fields in the solar internetwork. Consistent with earlier claims (e.g., Orozco Suárez & Bellot Rubio 2012; Borrero & Kobel, in preparation), the distribution of inclinations deviates significantly from a cosine function, and

<sup>3</sup> By this choice we ensure that the maximum possible information is used to infer the vector magnetic field. Nearly 100% of the 10,419 pixels with significant linear polarization signals also have Stokes V signals above the  $4.5\sigma$  threshold, meaning that four non-zero Stokes parameters are contributing to the determination of the vector magnetic field. The converse is not true: 39% of the pixels showing Stokes V amplitudes larger than  $4.5\sigma$  do not have linear polarization signals above  $4.5\sigma$ . Since the inversion of these pixels might not be as accurate as that of the other pixels, we refrain from including them in the analysis. We note, however, that the results derived from all the pixels with Stokes Q, U or V signals above  $4.5\sigma$  are fully compatible with the ones presented in this paper, in particular the field distributions of Figure 6: the inclination distribution still shows a pronounced—albeit slightly smaller—peak at  $90^\circ$ , and the field strength distribution is shifted to weaker fields by about 20 G. Those results account for 92.2% of the area covered by the internetwork.

<sup>4</sup> These values have been obtained as the strength of the vertical (horizontal) fields that produce circular (linear) polarization signals of  $1\sigma$  with the mean thermodynamic parameters of the quiet Sun.

<sup>5</sup> The  $4.5\sigma$  polarization threshold adopted for Stokes Q and U corresponds to a transverse field of 32 G, which is very far from the maximum of the distribution at 110 G. For this reason, we consider it unlikely that the peak is an artifact of the selection criteria.

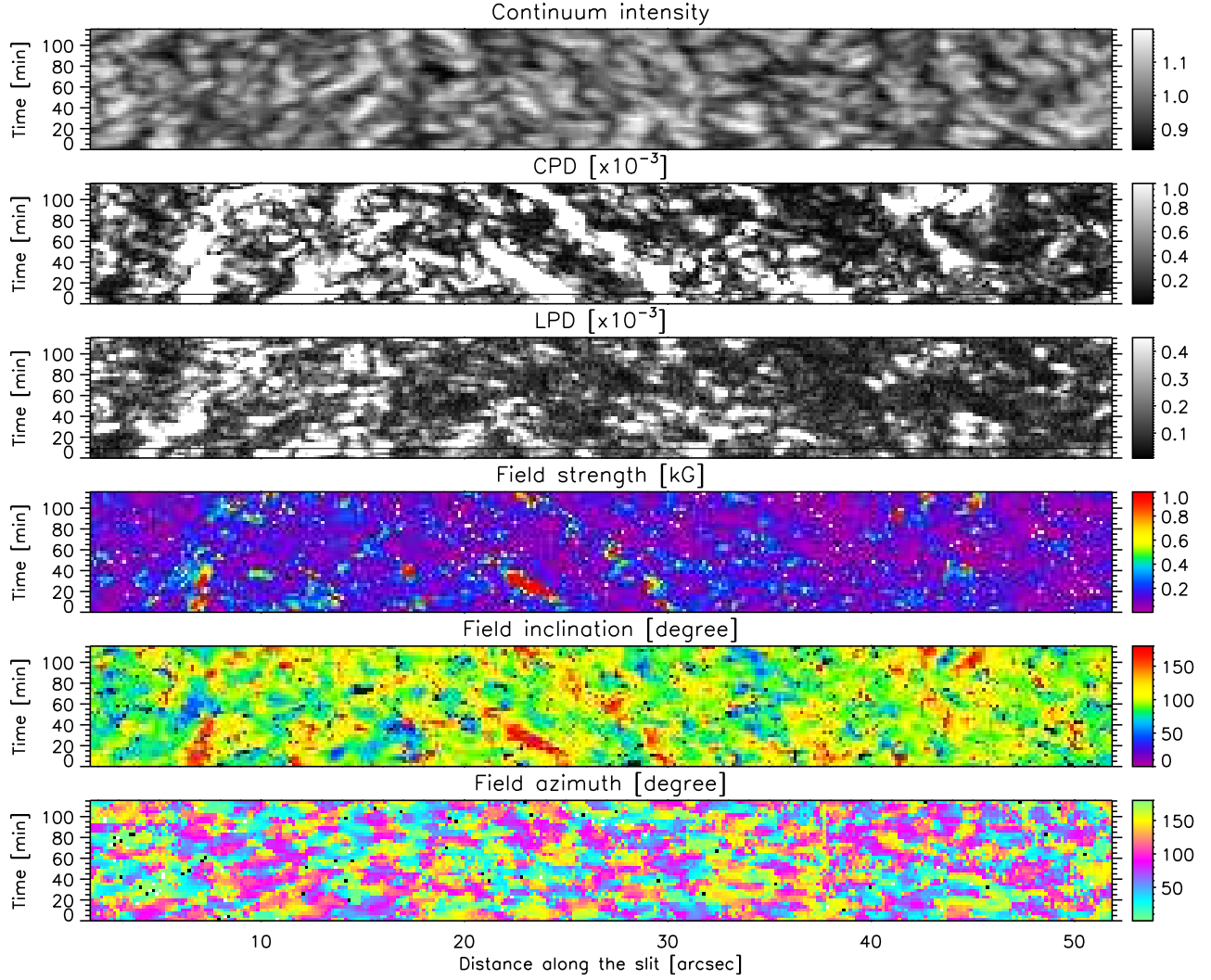


**Figure 4.** From top to bottom: temporal evolution of the observed continuum intensity, mean circular polarization degree, mean linear polarization degree, and field strengths, inclinations, and azimuths determined from the inversion. The horizontal and vertical directions represent distance along the slit and time (increasing from bottom to top), respectively. Only a fraction of the total slit length is shown to emphasize the spatial and temporal coherence of the signals. For display purposes, the Stokes spectra used to construct this figure were obtained through a running average of 6.1 minutes shifted by 3 minutes. The mean circular and linear polarization degrees have been computed using the two lines as  $[\sum_{i=1}^N |V(\lambda_i)|/I(\lambda_i)]/N$  and  $\sum_{i=1}^N \sqrt{Q(\lambda_i)^2 + U(\lambda_i)^2}/I(\lambda_i)]/N$ , respectively.  $N$  is the number of wavelength samples. The thin horizontal lines in the circular and linear polarization maps mark the position of the cuts shown in Figure 5.

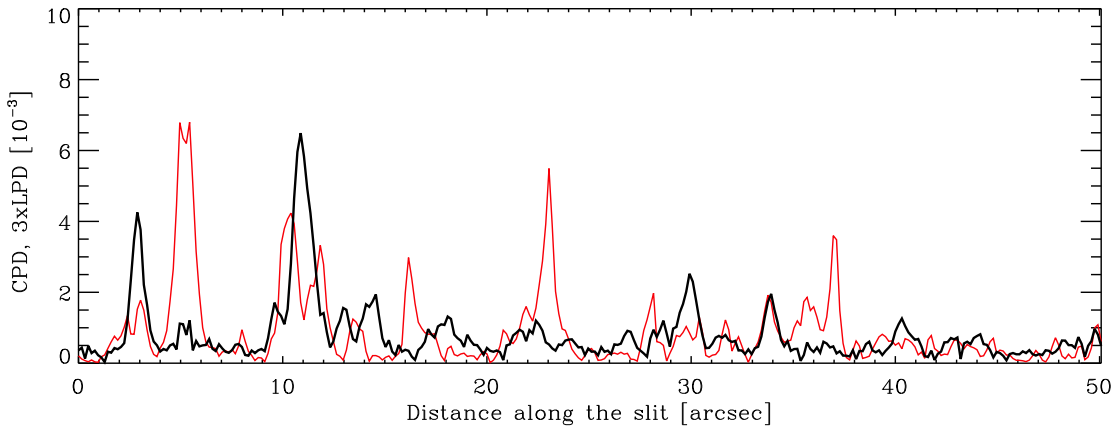


**Figure 5.** Horizontal cuts of the circular and linear polarization maps shown in Figure 4 at  $t = 12$  minutes (thin and thick lines, respectively). The exact position of the cuts is indicated by horizontal black lines in the second and third panels of Figure 4. The linear polarization signal has been multiplied by a factor of three for better visualization. These cuts demonstrate that the sizes of individual patches along the spatial direction are comparable in linear and circular polarization.

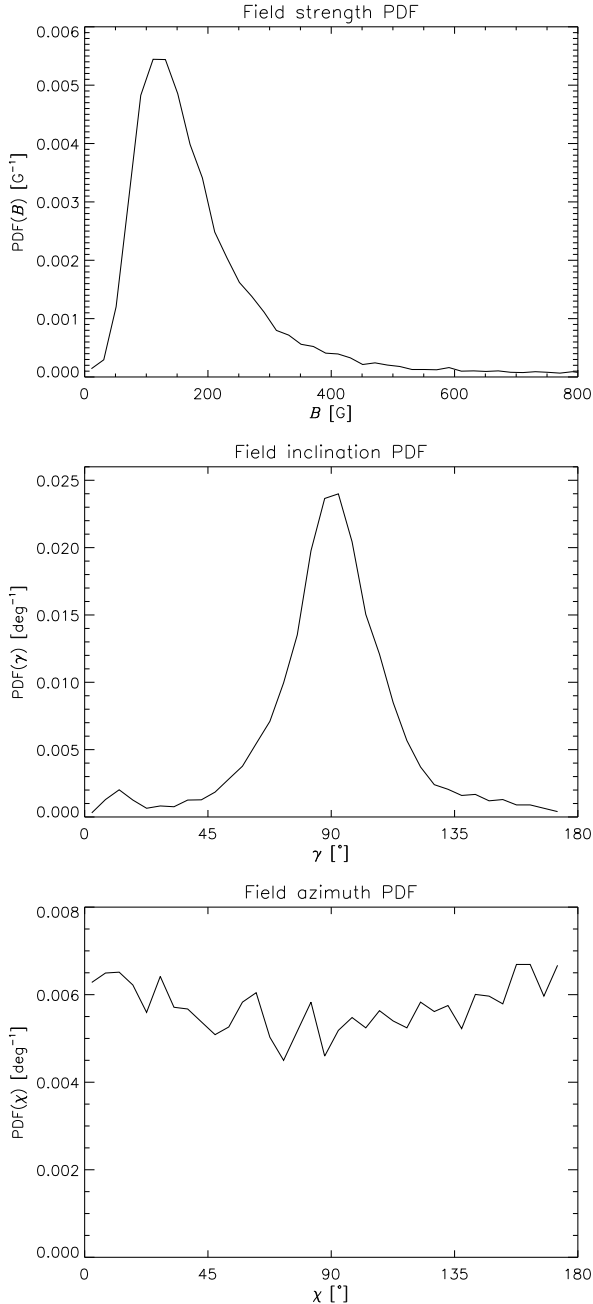


**Figure 6.** Distributions of magnetic field strengths, inclinations, and azimuths resulting from the inversion of pixels with linear polarization (Stokes Q or U) signals larger than 0.059% (4.5 times the noise level) in the ultra-deep SP maps averaged over 6.1 minutes. These PDFs account for 53% of the observed field of view.

therefore does not appear to be isotropic.

Finally, the PDF of field azimuth shows a random distribution of orientations in the solar surface.

## 5. DISCUSSION AND CONCLUSIONS

By pushing the integration time to a limit, the spectropolarimetric measurements taken by the *Hinode* SP reveal a quiet-Sun internetwork full of linear polarization signals. At least 69% of the area occupied by the internetwork shows unambiguous Stokes Q or U signals in the Fe I 630 nm lines when the noise is decreased down to  $7 \times 10^{-5} I_c$ . This, however, is

a difficult endeavor, requiring integrations of about 25 minutes which degrade the spatial resolution of the observations. With integrations of 10 minutes (comparable to the granular lifetime), the degradation is not so severe and 60% of the internetwork still shows measurable linear polarization. Similar coverage levels have been reported earlier from near-infrared Fe I 1565 nm measurements, but at lower spatial resolution (Martínez González et al. 2008; Beck & Rezaei 2009).

The origin of these signals is unclear as yet. They are pervasive, so the mechanism producing them must operate all over the solar surface. The observations are compatible with the existence of an “ocean” of weak and highly inclined fields which are present everywhere and can only be detected when the noise is reduced below a certain level—a true photospheric magnetic carpet. At the same time, it is possible that part of the observed Stokes Q and U signals come from transient *Horizontal Internetwork Fields* (HIFs; Lites et al. 1996, Ishikawa & Tsuneta 2009, Danilovic et al. 2010) and small-scale magnetic loops that emerge in the solar photosphere and progress into higher layers or disappear there (Centeno et al. 2007; Martínez González & Bellot Rubio 2009; Gömöry et al. 2010; Ishikawa et al. 2010; Martínez González et al. 2010). In fact, short-lived, localized HIFs emerging at high rates can be expected to completely fill the slit with signals for long enough integrations (a similar conclusion was reached by Ishikawa & Tsuneta 2010 from the analysis of deep vector magnetograms taken with the *Hinode* Narrowband Filter Imager). The only way to distinguish between scenarios is to investigate the time evolution of the fields at high cadence and very low noise levels. This task should be performed by the new generation of large ( $> 1.5\text{m}$ ) telescopes, including NST, GREGOR, and, on the longer term, also ATST, EST, and Solar-C.

We have used the deep *Hinode* integrations to derive the properties of internetwork fields through a Milne–Eddington inversion with constant atmospheric parameters and a local non-magnetic component. To avoid excessive degradation of the spatial resolution and large variations of the solar conditions, we use Stokes spectra integrated for 6.1 minutes, comparable to the mean granular lifetime. Only pixels showing Stokes Q or U signals above 4.5 times the noise level ( $1.3 \times 10^{-4} I_c$ ) were considered for analysis. They represent 53% of the solar internetwork. These pixels also have significant circular polarization signals, so the magnetic field parameters derived from the inversion are very accurate because all the available information is used at the same time (Asensio Ramos 2009; Borrero & Kobel 2011). Our threshold of 4.5 times the noise level is rather strict, but designed to pick only real signals. The probability that a random variable following a normal distribution of zero mean and standard deviation  $\sigma$  exceeds  $4.5\sigma$  is  $7 \times 10^{-6}$ . Thus, the probability that a pixel without any linear polarization is selected erroneously would be  $7 \times 10^{-6} \times 90 \times 2 = 0.0013$ , since 90 wavelengths are used to determine the maximum of the polarization profile and there are 2 of them (Stokes Q and U). With such a low probability, one can be completely sure that the inverted profiles are real and not artifacts of the noise.

The magnetic field distributions inferred from the inversion confirm that internetwork fields are weak and very inclined. The peaks of field strength and inclination occur at 110 G and  $90^\circ$ , respectively, as had been estimated from noisier observations in the past (Orozco Suárez et al. 2007b;

Orozco Suárez & Bellot Rubio 2012). The field inclination distribution is not isotropic and does not consist only of purely horizontal fields, since there exist a non-negligible amount of pixels with inclinations between  $45^\circ$  and  $90^\circ$  (or between  $90^\circ$  and  $135^\circ$ ). Finally, the field azimuth appears to be randomly oriented, as required to explain the absence of Stokes U signals in Hanle-effect measurements of spectral lines near the limb (e.g., Stenflo 1982).

Because of their very similar properties (weak strengths near or below the Hanle saturation limit, large inclinations, random orientation of azimuths, and almost complete coverage of the solar surface), it is tempting to speculate that the magnetic fields revealed by the long integrations of *Hinode* are those sampled by Hanle-depolarization measurements. In the future, progress will come from the observation of the temporal evolution of internetwork fields, including their emergence and disappearance in the solar atmosphere. With current instruments, such observations are not feasible due to insufficient photon collecting power. This limitation highlights the need for larger telescopes, both on the ground and in space.

This work has been funded by the Spanish MICINN through projects AYA2011-29833-C06-04 and PCI2006-A7-0624, and by Junta de Andalucía through project P07-TEP-2687, including a percentage from European FEDER funds. D.O.S. thanks the Japan Society for the Promotion of Science (JSPS) for financial support through its postdoctoral fellowship program for foreign researchers. *Hinode* is a Japanese mission developed and launched by ISAS/JAXA, with NAOJ as domestic partner and NASA and STFC (UK) as international partners. It is operated by these agencies in cooperation with ESA and NSC (Norway). The use of NASA's Astrophysical Data System is gratefully acknowledged.

## REFERENCES

- Alissandrakis, C. E., Dialetis, D., & Tsiropoula, G. 1987, *A&A*, 174, 275  
 Asensio Ramos, A. 2009, *ApJ*, 701, 1032  
 Barthol, P., Gandorfer, A., Solanki, S. K., et al. 2011, *Sol. Phys.*, 268, 1  
 Beck, C., & Rezaei, R. 2009, *A&A*, 502, 969  
 Borrero, J. M., & Kobel, P. 2011, *A&A*, 527, A29  
 Centeno, R., Socas-Navarro, H., Lites, B., et al. 2007, *ApJ*, 666, L137  
 Gömöry, P., Beck, C., Balthasar, H., et al. 2010, *A&A*, 511, A14  
 Danilovic, S., Beeck, B., Pietarila, A., et al. 2010, *ApJ*, 723, L149  
 del Toro Iniesta, J. C., Orozco Suárez, D., & Bellot Rubio, L. R. 2010, *ApJ*, 711, 312  
 Gošić, M. 2012, Master Thesis, University of Granada (Spain)  
 Hinzberger, J., Bonet, J. A., Vázquez, M., & Hanslmeier, A. 1999, *ApJ*, 515, 441  
 Ichimoto, K., Lites, B., Elmore, D., et al. 2008, *Sol. Phys.*, 249, 233  
 Ishikawa, R., & Tsuneta, S. 2009, *A&A*, 495, 607  
 Ishikawa, R., & Tsuneta, S. 2010, *ApJ*, 718, L171  
 Ishikawa, R., Tsuneta, S., & Jurčák, J. 2010, *ApJ*, 713, 1310  
 Khomenko, E. V., Martínez González, M. J., Collados, M., et al. 2005, *A&A*, 436, L27  
 Kosugi, T., Matsuzaki, K., Sakao, T., et al. 2007, *Sol. Phys.*, 243, 3  
 Lites, B. W. 1996, *Sol. Phys.*, 163, 223  
 Lites, B. W., & Socas-Navarro, H. 2004, *ApJ*, 613, 600  
 Lites, B. W., Elmore, D. F., & Ständer, K. V. 2001, in *ASP Conf. Proc.*, Vol. 236, *Advanced Solar Polarimetry - Theory, Observation, and Instrumentation*, ed. M. Sigwarth (San Francisco, CA: ASP), 33  
 Lites, B. W., Kubo, M., Socas-Navarro, H., et al. 2008, *ApJ*, 672, 1237  
 Lites, B. W., Leka, K. D., Skumanich, A., Martínez Pillet, V., & Shimizu, T. 1996, *ApJ*, 460, 1019  
 Martínez González, M. J., Collados, M., Ruiz Cobo, B., & Beck, C. 2008, *A&A*, 477, 953  
 Martínez González, M. J., & Bellot Rubio, L. R. 2009, *ApJ*, 700, 1391  
 Martínez González, M. J., Manso Sainz, R., Asensio Ramos, A., & Bellot Rubio, L. R. 2010, *ApJ*, 714, L94  
 Martínez Pillet, V., et al. 2011, *Sol. Phys.*, 268, 57  
 Orozco Suárez, D., Bellot Rubio, L. R., & del Toro Iniesta, J. C. 2007a, *ApJ*, 662, L31  
 Orozco Suárez, D., Bellot Rubio, L. R., & del Toro Iniesta, J. C. et al. 2007b, *ApJ*, 670, L61  
 Orozco Suárez, D., Bellot Rubio, L. R., & del Toro Iniesta, J. C. et al. 2007c, *PASJ*, 59, 837  
 Orozco Suárez, D., & Bellot Rubio, L. R. 2012, *ApJ*, 751, 2  
 Sainz Dalda, A., Martínez-Sykora, J., Bellot Rubio, L., & Title, A. 2012, *ApJ*, 748, 38  
 Shimizu, T., Nagata, S., Tsuneta, S., et al. 2008, *Sol. Phys.*, 249, 221  
 Socas-Navarro, H., Borrero, J. M., Asensio Ramos, A., et al. 2008, *ApJ*, 674, 596  
 Solanki, S. K., et al. 2010, *ApJ*, 723, L127  
 Stenflo, J. O. 1982, *Sol. Phys.*, 80, 209  
 Suematsu, Y., Tsuneta, S., Ichimoto, K., et al. 2008, *Sol. Phys.*, 249, 197  
 Title, A. M., Tarbell, T. D., Topka, K. P., et al. 1989, *ApJ*, 336, 475  
 Tsuneta, S., Ichimoto, K., Katsukawa, Y., et al. 2008, *Sol. Phys.*, 249, 167  
 Vitićhić, B., Sánchez Almeida, J., Del Moro, D., & Berrilli, F. 2011, *A&A*, 526, A60  
 Vitićhić, B., & Sánchez Almeida, J. 2011, *A&A*, 530, A14